Hindawi
Mathematical Problems in Engineering
Volume 2019, Article ID 1016261, 12 pages
https://doi.org/10.1155/2019/1016261

Research Article

Pedestrian Delay Model for Continuous Flow Intersections under Three Design Patterns

Tao Wang,[1] Jing Zhao ,[2] and Chaoyang Li[1]

[1]*School of Naval Architecture, Ocean & Civil Engineering, Shanghai Jiao Tong University, Shanghai 200240, China*
[2]*Department of Traffic Engineering, University of Shanghai for Science and Technology, Shanghai 200093, China*

Correspondence should be addressed to Jing Zhao; jing_zhao_traffic@163.com

Received 30 November 2018; Accepted 16 January 2019; Published 23 January 2019

Academic Editor: F. R. B. Cruz

In order to accurately evaluate the level of service of pedestrians and provide the basis for the optimized design, the pedestrian delay of the continuous flow intersection was analyzed. According to the characteristics of streams of pedestrians' arriving and leaving, the pedestrian delay models of different directions (namely, straight and diagonal) were established for three pedestrian passing patterns of the continuous flow intersection. The accuracy of the models was verified by VISSIM. The deviation was less than 3%. The effects of three key factors, namely, the vehicle demands, pedestrian demands and percentage of diagonal crossing, on the delay of the pedestrian under three modes were discussed by sensitivity analysis. The results show that the traditional pedestrian passing pattern mainly applies on the conditions that vehicle and pedestrian demands are low. The pattern of interspersed pedestrian passing is mainly applicable to the conditions of high vehicle and pedestrian demands. Although the pattern of exclusive pedestrian passing phase was least selected as the optimal design, it can apply to traffic demand fluctuating condition for its insensitive to volume and pedestrian demand pattern.

1. Introduction

The intersection is the bottleneck node of the urban road network, in which the traffic problems are mainly caused by the complicated traffic flow. To better deal with the conflict between left-turn and through vehicles, a series of unconventional intersection designs were proposed, including median U-turn intersections [1, 2], superstreet intersections [1, 3, 4], uninterrupted flow intersections [5], special width approach lanes [6], dynamic reversible lane control [7], displaced left-turn intersections [8, 9], exit-lanes for left-turn intersections (EFL) [10–12], and tandem intersections [13–15].

The continuous flow intersection (CFI) is one of these unconventional intersections, which was first proposed by Mier [16]. It can eliminate the conflict between left-turn and through vehicles at the main signal by transferring the conflict point between the left-turn vehicles and opposite through vehicles to the upstream presignal, so that the capacity of intersections will be improved. A series of theoretical research and practical tests about CFI have been carried out, including geometric design, signal control, and operational evaluation. The CFI has been taken into application in real life in many countries [17], such as United States, Australia, and China.

From the perspective of the geometric design, Inman [18] studied the traffic sign and lane marking system of the continuous flow intersection to improve its visual recognition based on driving simulator experiments. Hughes [17] gave a series of detailed suggestions on layout design, including left-turn lane length, presignal intersection width, turning radius, and other detail structure at continuous flow intersections. The distances between the main signal and presignal under different traffic demands were further recommended by Tanwanichkul [19] based on the operational efficiency comparison under different distances between the main signal and the presignal using the VISSIM simulation.

From the perspective of signal control, Tarko [20] developed the basic strategy of signal timing according to the traffic characteristics of continuous flow intersections. On this basis, considering the conditions of the balance and unbalance of traffic flow in each approach and exit lane, Esawey [21] proposed a signal control method composed of six phases

and realized it by Synchro software. Zhao [22, 23] established an integrated optimization model for the geometric layout and signal timing in which many key parameters, such as intersection form, lane function, left-turn lane length, and signal timing, were optimized in a unified framework.

From the perspective of operational evaluation, Chang et al. developed a well-calibrated CFI traffic simulators using VISSIM to evaluate the operational properties under various constraints and traffic conditions, which can assist engineers in identifying potential bottlenecks and estimating delays for CFI designs at the planning stage [24]. Moreover, in practice, the average waiting time of vehicles decreased by 50% and the traffic capacity increased by 31% after the continuous flow intersections of Utah's 3500 South Highway and Bangerter Highway opened to the public in 2007, which further verified the practical significance of continuous flow intersections [25].

The above research on continuous flow intersections mainly focuses on vehicles. However, in developing countries, walking is an important travel mode [26–28], so it is a necessary condition for its application in developing countries to deal with pedestrian crossing street at continuous flow intersections. For this, Jagannathan [29] proposed a new design for pedestrians, namely, interlaced crossing. The performance of vehicles and pedestrians was discussed based on Vissim simulation, in which the signal timing was optimized for vehicular traffic performance. Coates [30] further proposed a flexible signal control program under the interlaced pedestrian crossing design to reduce vehicle delay while prioritizing pedestrian crossing. The signal control procedure dynamically chooses the appropriate phase and green time combination to minimize delay by considering pedestrian wait time and existing queue length. However, these studies did not provide in-depth discussions about pedestrian delay at continuous flow intersections.

A series of calculation models for pedestrian delay at conventional intersections have been established in the past. One commonly used pedestrian delay model is the one presented in the highway capacity manual (HCM) [31]. It is a function of the ratio of the length of the pedestrian effective green time and the length of the signal cycle for one-stage crossings based on uniform arrival rates. Based on this model, many influencing factors were deeply analyzed by researchers to enhance the accuracy of the calculation model. These factors include the pedestrian-vehicle conflict considering the variety of the motorist yielding behavior [32], the pedestrians' arrival rate considering the irregularity of the pedestrians' arrival rate [33–35], the signal noncompliance considering pedestrians who entered crosswalks during clearance phases or red phases [36–39], the information of remaining green time [40], the two-stage crossing design considering the effect of the signal timing at the first-stage crossing on the pedestrian arrivals at the second-stage crossing [41, 42], and the bidirectional pedestrian flow considering the opposing pedestrian flow on the walking speed [43, 44].

Pedestrian service level is an important factor for the application of continuous flow intersections on urban roads. At present, the research on continuous flow intersections mainly focuses on vehicles and the evaluation of pedestrian delay is mainly based on simulation, which limits the application, especially in developing countries. Therefore, this paper aims to establish a calculation model of pedestrian delay at CFI, in which three design patterns of pedestrian crossing are considered. Considering the proposed delay models can be used to provide the guidance for engineering practice in the future, all possible pedestrian crossing patterns are discussed, even though some of them have not been taken into practice in the real world.

The rest of the paper is organized as follows. In Section 2, the three design patterns of pedestrian crossing at CFI are described. The detailed pedestrian delay calculation model is established in Section 3. The proposed model is validated in Section 4. The sensitivity of the key parameters in the proposed model is discussed in Section 5. Conclusions and recommendations are given at the end.

2. Design Patterns of Pedestrian Crossing at CFI

The basic geometric design concept of continuous flow intersection is shown in Figure 1(a). The presignal is set at the upstream of the intersection so that left-turn vehicles can be guided to the left of opposite traffic flow, which can eliminate the conflicts between left-turn and opposite through vehicles at the main signals. Therefore, the two-phase signal plan can be used in the main-signal and presignals. Combining the main-signal and presignals, the CFI can run under a six-phase plan, as illustrated in Figure 1(b).

For the pedestrians, there are three design patterns, namely, the conventional pattern, the exclusive phase pattern, and the interlaced crossing pattern.

Under the conventional pattern (pattern 1), the pedestrians cross the CFI as the same way as the conventional intersections, as shown in Figure 2. There are conflicts between pedestrians and left/right turn vehicles when pedestrians are crossing the intersection at the green light through vehicles, because the continuous flow intersection runs in two phases at the main signal.

Under the exclusive phase pattern (pattern 2), the pedestrians can only cross the street during the exclusive phase, as shown in Figure 3. The exclusive phase for pedestrians is added on the basis of two phases for vehicles at the main signal. Pedestrians can cross the intersection in each direction (including diagonally) without any conflicts.

Under the interlaced crossing pattern (pattern 3), the pedestrians can cross the intersection between through vehicles in the same direction and left-turn vehicles in the opposite direction on the designed crosswalk, as shown in Figure 4. By this way, the conflicts between pedestrian and left-turn vehicles can be eliminated while pedestrians crossing the street will be retarded by multiple signals.

3. Pedestrian Delay Model Establishment

3.1. Model Parameters. To facilitate the model presentation, the notations used hereafter are summarized in Table 1.

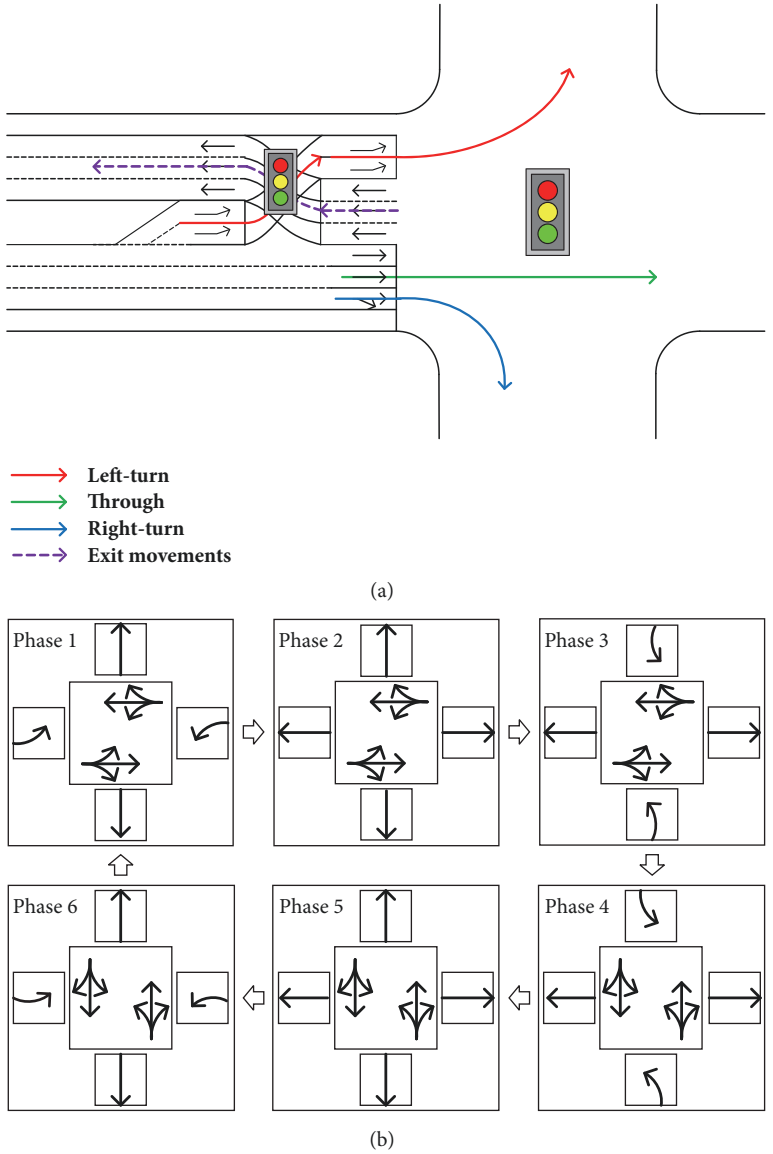

Figure 1: Concept of CFI. (a) Geometric design. (b) Phase plan.

3.2. Pedestrian Delay Model under Conventional Crossing Pattern. There are two aspects of pedestrian delay in this pattern, including (1) delay caused by signal control: pedestrians have to wait at the roadside due to the pedestrian phase, which leads to signal delay; (2) delay caused by conflicts: pedestrians must pass through conflict zones of left-right turning vehicles, which causes conflict delays.

(1) Delay Caused by Signal Control. Under the conventional crossing pattern, only the through movement of pedestrian is allowed. The diagonal movement can be accomplished by crossing the street twice. Therefore, the through and diagonal movement have to meet the signal control once and twice, respectively. The calculation diagrams of the two conditions are shown in Figures 5 and 6, respectively.

For through movement, as shown in Figure 5, the segment "AC" represents the arrival of pedestrians to the intersection and its slope is the arriving rate. The segment "BC" represents the departure of pedestrians at the beginning of the green phase and its slope is the saturation flow rate. The segment "BD" is the pedestrian dissipation time. The area of the shadow triangle "ABC" is the total pedestrian delay, which can be calculated by (1). The length of segments "AB" and "CD" can be calculated by (2) and (3), respectively. Therefore, the average pedestrian delay of signal control can be calculated by (4).

$$S = \frac{l_{AB} l_{CD}}{2} \tag{1}$$

$$l_{AB} = r \tag{2}$$

$$l_{CD} = \frac{s q_1 r}{(s - q_1)} \tag{3}$$

$$d_{s11} = \frac{S_{ABC}}{Cq} = \frac{sr^2}{2C(s - q_1)} \tag{4}$$

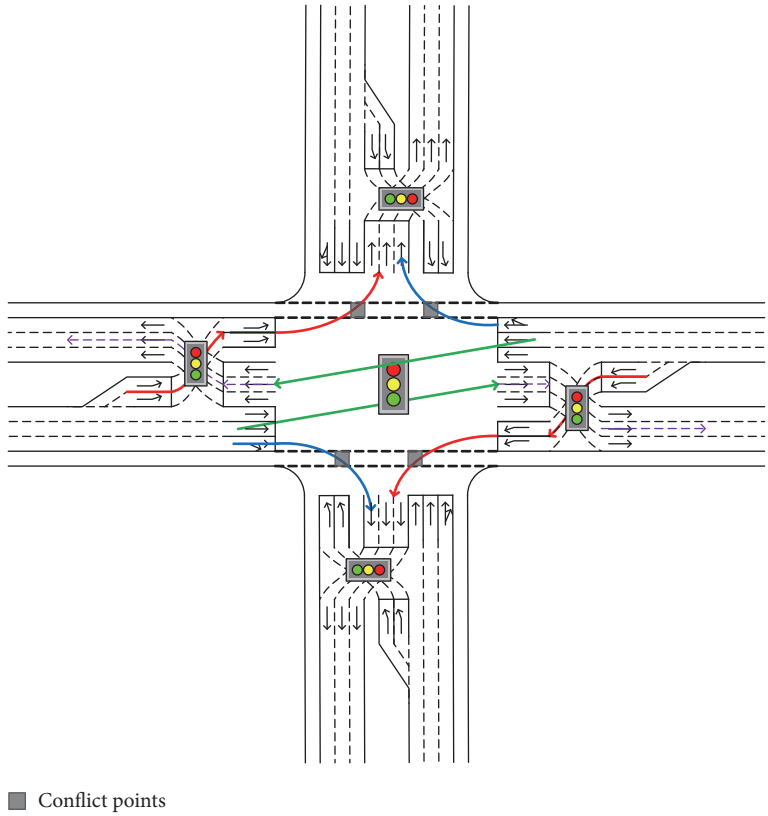

Figure 2: Conventional pattern.

For diagonal movement, as shown in Figure 5, the segment "AD" represents the arrival of pedestrians to the intersection. The segment "BC" represents the departure of pedestrians at the beginning of the green phase. The segment "EFG" represents the arrival of pedestrians to the second stage of crossing. The segment "HI" represents the departure of pedestrians at the beginning of the green phase along the crossing street. The length of horizontal segment in triangle "ABC" denotes the delay when pedestrians waiting for green light at the first stage of crossing; the length of horizontal segment in polygon "BCDEFG" denotes the pedestrian walking time on the crosswalk; the length of horizontal segment in polygon "EFGHI" denotes the delay when pedestrians waiting for green light at the second stage of crossing. Therefore, the area of the shadow part is the total pedestrian delay, which can be calculated by (5). The length of segments "AB", "GH", "EI", and "IK" can be calculated by (6), (7), (8), and (9), respectively. Therefore, the average pedestrian delay of signal control can be calculated by (10).

$$S = \frac{(l_{AB} + l_{GH} + l_{EI})\, l_{IK}}{2} \tag{5}$$

$$l_{AB} = r \tag{6}$$

$$l_{GH} = t_b - t_w \tag{7}$$

$$l_{EI} = t_b - t_w - g + \frac{Cq}{s} \tag{8}$$

$$l_{IK} = Cq \tag{9}$$

$$d_{s12} = \frac{r}{2} + t_b - t_w - \frac{g}{2} + \frac{Cq}{2s} \tag{10}$$

(2) Delay Caused by Conflicts. The delay caused by conflicts is directly related to the left-turn and right-turn traffic flow and the distance distribution between vehicles, which can be calculated according to the equation in the literature [45]. Therefore, the delay caused by conflicts for through movement and diagonal movement can be calculated by (11) and (12), respectively, in which the acceptable gap for pedestrians to cross, τ, can be calculated by (13) [45].

$$d_{c11} = \frac{1/\lambda - (\tau + 1/\lambda)\, e^{-\lambda\tau}}{e^{-\lambda\tau}} \tag{11}$$

$$d_{c12} = \frac{1/\lambda - (\tau + 1/\lambda)\, e^{-\lambda\tau}}{e^{-\lambda\tau}} + \frac{1/\lambda' - \left(\tau + 1/\lambda'\right) e^{-\lambda'\tau}}{e^{-\lambda'\tau}} \tag{12}$$

$$\tau = \frac{W}{v_p} + t_p + t_0 \tag{13}$$

Combining the delay caused by signal control and the delay caused by conflicts, the pedestrian delay under conventional crossing pattern can be calculated by (14).

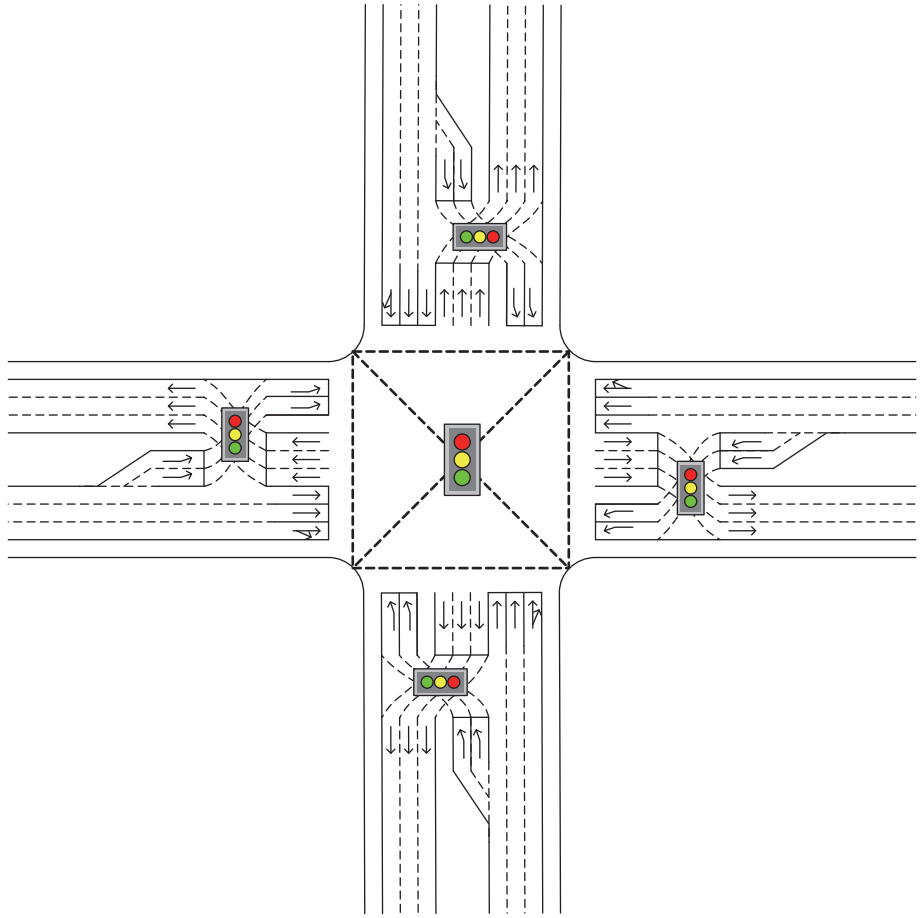

Figure 3: Exclusive phase pattern.

$$d_1 = \frac{\sum_{j=1}^{2} q_j \left(d_{s1j} + d_{c1j}\right)}{\sum_{j=1}^{2} q_j} \tag{14}$$

3.3. Pedestrian Delay Model under Exclusive Phase Pattern. Pedestrians have exclusive phases so that the through and diagonal pedestrians can cross the street simultaneously, and its delay is only caused by signal control which can be illustrated by Figure 5. The shadow triangle abc is the total pedestrian delay and the calculation equation of average pedestrian delay is shown in (15).

$$d_2 = \frac{\sum_{j=1}^{2} \left(sq_j r^2 / 2C\left(s - q_j\right)\right)}{\sum_{j=1}^{2} q_j} \tag{15}$$

3.4. Pedestrian Delay Model under Interlaced Crossing Pattern. Pedestrian delay in this pattern is mainly caused by signal control and conflict delay of right-turn vehicles.

(1) Delay Caused by Signal Control. The setting of interlaced crosswalk is illustrated in Figure 7. Under the interlaced crossing pattern, the through and diagonal movement have to meet the signal control twice and thrice, respectively. The calculation diagrams of the two conditions are shown in Figures 6 and 8, respectively.

For through movement, pedestrians should meet the signal control twice. For easy discussion, using the route from point 1 to point 4 in Figure 7 as an example, pedestrians have to wait for green signal of the east-west direction at point 1 and wait for green signal of the south-north direction at point 3. As shown in Figure 6, the segment "AD" represents the arrival of pedestrians to point 1. The segment "BC" represents the departure of pedestrians at the beginning of the green phase. The segment "EFG" represents the arrival of pedestrians to point 3. The segment "HI" represents the departure of pedestrians at the beginning of the green phase along the crossing street. Therefore, the average pedestrian delay of signal control can be calculated by

$$d_{s31} = \frac{r}{2} + t_b - t_w - \frac{g}{2} + \frac{Cq}{2s} \tag{16}$$

For diagonal movement, pedestrians should meet the signal control thrice. For easy discussion, using the route from point 1 to point 6 in Figure 7 as an example, pedestrians have to wait for green signal of the east-west direction at point 1, wait for green signal of the south-north direction at point 3, and wait for green signal of the east-west direction at point 5. As shown in Figure 8, the area of the shadow part is the total pedestrian

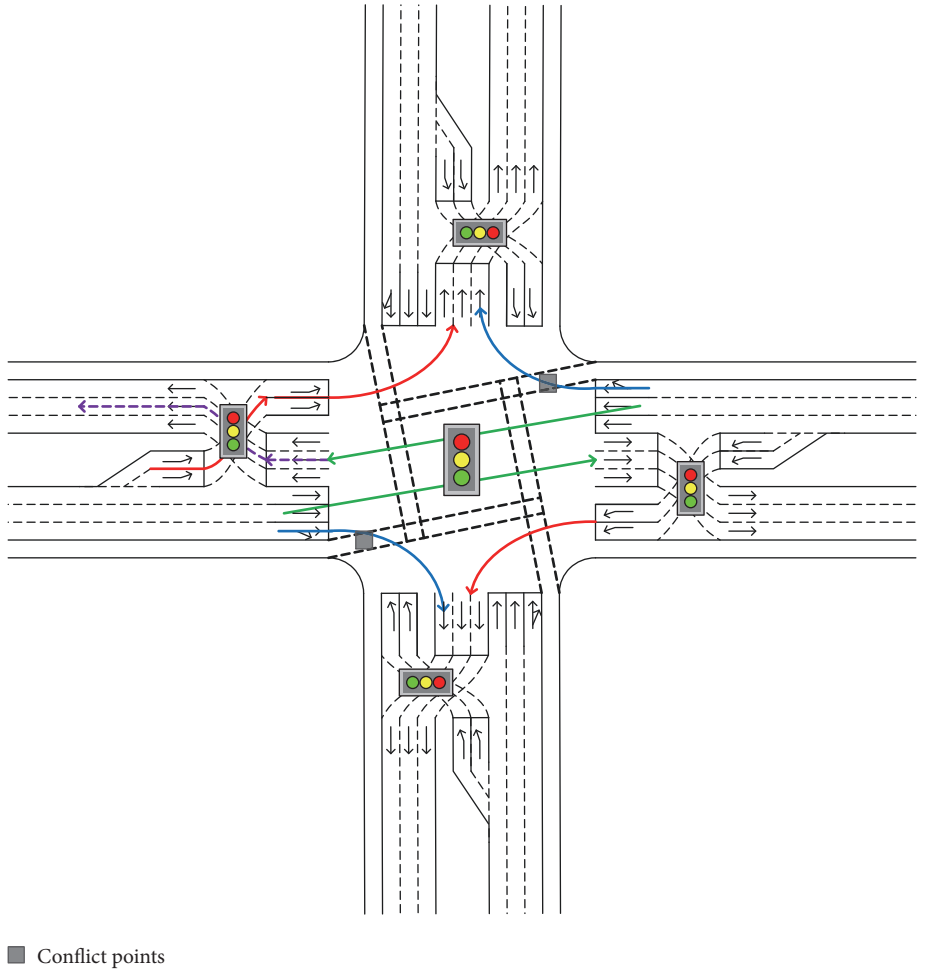

Figure 4: Interlaced crossing pattern.

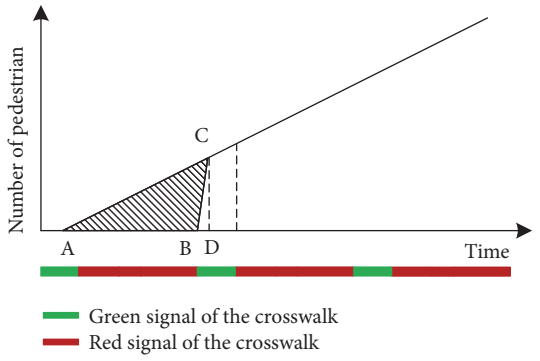

Figure 5: Calculation diagram for the pedestrians meeting the signal control once.

delay, which can be calculated by (17). The length of segments "AB", "GH", "KM", "EI", "JN", and "NK" can be calculated by (18), (19), (20), (21), (22), and (23), respectively. Therefore, the average pedestrian delay of signal control can be calculated by (24).

$$S = \frac{(l_{AB} + l_{GH} + l_{KM} + l_{EI} + l_{JN})\, l_{NO}}{2} \tag{17}$$

$$l_{AB} = r \tag{18}$$

$$l_{GH} = t_b - t_w \tag{19}$$

$$l_{KM} = t'_b - t'_w \tag{20}$$

$$l_{EI} = t_b - t_w - g + \frac{Cq}{s} \tag{21}$$

Table 1: Notations of key model parameters and variables.

Notation	Definition
i	Index of the design pattern, $i = 1, 2, 3$ for the conventional pattern, the exclusive phase pattern, and the interlaced crossing pattern, respectively
j	Index of pedestrian movements, $j = 1, 2$, represents through movement and diagonal movement respectively
C	Cycle length of the intersection, s
g	Green time of the crosswalk, s
r	Red time of the crosswalk, s
t_b	Interval from the start of green of the crosswalk to that of the crosswalk on the crossing street, s
t'_b	Interval from the start of green of the crosswalk on the crossing street to that of the crosswalk on the studied street, s
t_w	Walking time on the crosswalk, s
t'_w	Walking time on the crosswalk on the crossing street, s
t_p	Waiting time for pedestrian to decide whether to cross, s
t_0	Passing time of vehicle, s
τ	Acceptable gap for pedestrians to cross, s
q_1, q_2	Arriving rate of pedestrian for through movement and diagonal movement, respectively, ped/s
s	Saturation rate of pedestrian, ped/s
W	Width of one vehicle lane, m
v_p	Speed of pedestrian crossing the street, m/s
λ	Arriving rate of conflicting vehicles, veh/s
λ'	Arriving rate of conflicting vehicles on the crossing street, veh/s
l	Length of the segment in the calculation diagrams
S	Area of the shadow in the calculation diagrams
d_{sij}	Delay caused by signal control for pedestrian movement j under design pattern i, s
d_{cij}	Delay caused by conflicts for pedestrian movement j under design pattern i, s
d_i	Delay of pedestrian under design pattern i, s

$$l_{JN} = t'_b - t'_w \tag{22}$$

$$l_{NO} = Cq \tag{23}$$

$$d_{s32} = \frac{r}{2} + t_b - t_w - \frac{g}{2} + \frac{Cq}{2s} + t'_b - t'_w \tag{24}$$

(2) Delay Caused by Signal Control. The calculation principle of the delay caused by signal control under this design pattern is the same as the conventional crossing pattern. Therefore, the delay caused by right-turn vehicles can be calculated by

$$d_{c31} = \frac{1/\lambda - (\tau + 1/\lambda)\, e^{-\lambda\tau}}{e^{-\lambda\tau}} \tag{25}$$

$$d_{c32} = \frac{1/\lambda - (\tau + 1/\lambda)\, e^{-\lambda\tau}}{e^{-\lambda\tau}} + \frac{1/\lambda' - \left(\tau + 1/\lambda'\right) e^{-\lambda'\tau}}{e^{-\lambda'\tau}} \tag{26}$$

Combining the delay caused by signal control and the delay caused by conflicts, the pedestrian delay under conventional crossing pattern can be calculated by

$$d_3 = \frac{\sum_{j=1}^{2} q_j \left(d_{s3j} + d_{c3j}\right)}{\sum_{j=1}^{2} q_j} \tag{27}$$

4. Model Validation

The accuracy of models was tested by VISSIM simulation. The geometric design of CFI to be tested is shown in Figure 9. The distance of the main signal and presignal is 100 m. The pedestrian speed is 1.2 m/s. The pedestrian volume is 720 ped/h (the arriving rate is 0.2 ped/s). The saturation flow rate of the crosswalk is 8 ped/s. The traffic volume of is shown in Table 2. The average pedestrian crossing delay can be measured by calculating the weighted average delay of all pedestrian crossing routes.

The experiment was simulated by VISSIM and the simulation results were then compared with the calculation results of the model proposed, as is shown in Figure 10. The average

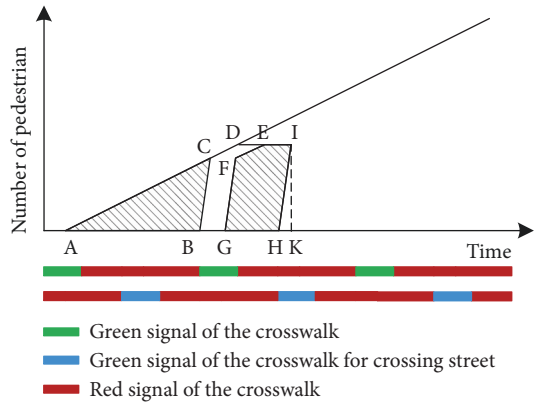

Figure 6: Calculation diagram for the pedestrians meeting the signal control twice.

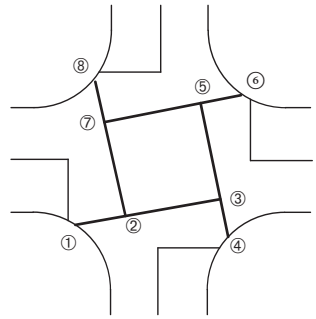

Figure 7: Setting of the interlaced crosswalk.

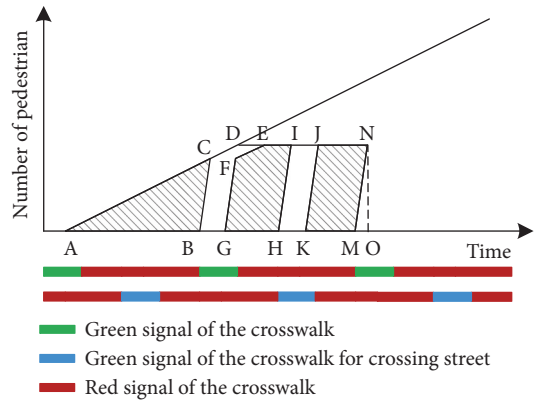

Figure 8: Calculation diagram for the pedestrians meeting the signal control thrice.

error for the conventional pattern (pattern 1), the exclusive phase pattern (pattern 2), and the interlaced crossing pattern (pattern 3) are 1.98 s, 1.24 s, and 2.56 s, respectively. Moreover, the results of paired t-test, as shown in Table 3, further show no significant difference between the results of the proposed model and that from simulation (p value = 0.363 > 0.05), which indicates the accuracy of the proposed pedestrian delay model is acceptable.

5. Sensitivity Analyses

The impact of three pedestrian crossing patterns on the delay of pedestrian is related to vehicular volume, pedestrian volume, and the proportion of diagonal crossing. The sensitivity analyses of the three design patterns were conducted below to further reveal the applicability of the three patterns.

The impact of vehicular volume on pedestrian delay is shown in Figure 11. The vehicular volume is changed from

Table 2: Traffic volume.

Movement	East leg	West leg	South leg	North leg
Left-turn	900	800	800	900
Through	1100	1200	1200	1100
Right-turn	400	500	500	400
Total	2400	2500	2500	2400

Table 3: Paired t-test results.

Mean	Std. deviation	Std. error mean	95% Confidence interval of the difference		t	df	Sig. (2-tailed)
			Lower	Upper			
0.310	1.528	0.333	-0.385	1.006	0.931	20	0.363

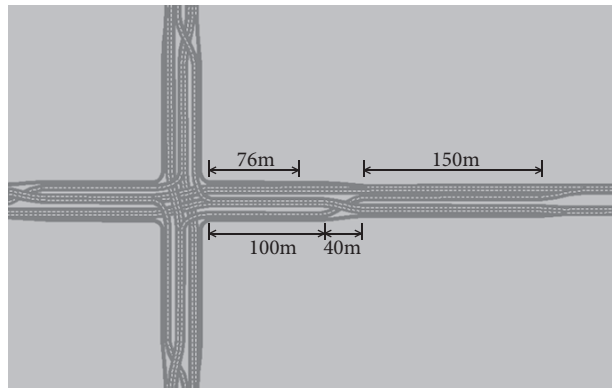

Figure 9: Geometric design of CFI.

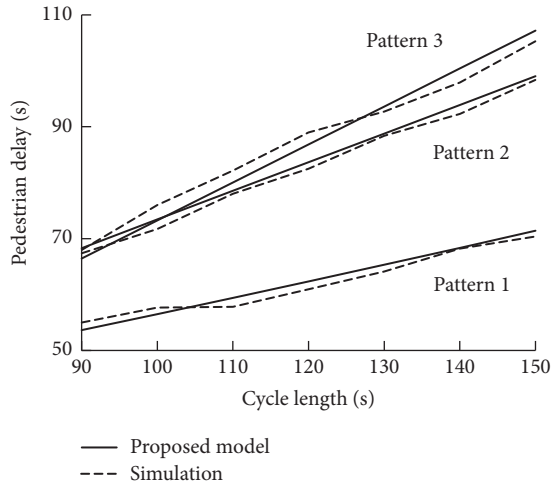

Figure 10: Geometric design of CFI.

300 veh/h/ln to 540 veh/h/ln. The pedestrian delays under the three patterns increase with the increase of vehicular volume. The conventional pattern is most affected and the exclusive phase pattern is least affected. In the condition of low vehicular volume (less than 380 veh/h/ln), the conventional pattern has the least pedestrian delay. It is due to the fact that there are lots of gap for pedestrians to cross in the vehicular flow when the volume is not high, so it is the most efficient for pedestrians to cross the street by using the gap between vehicles. However, in the condition of medium vehicular volume (between 380 and 480 veh/h/ln) the interlaced crossing pattern has the shortest average pedestrian delay. In the condition of high vehicular volume (more than 480 veh/h/ln), the exclusive phase pattern has the shortest average pedestrian delay, while the pedestrian delay of conventional pattern turns to be the longest. It is due to the fact that the

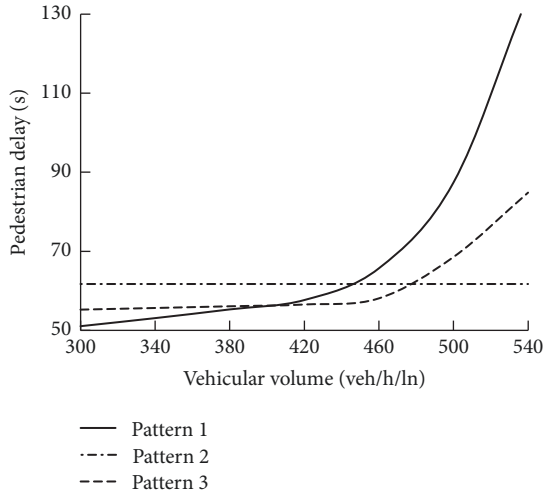

Figure 11: Impact of vehicular volume.

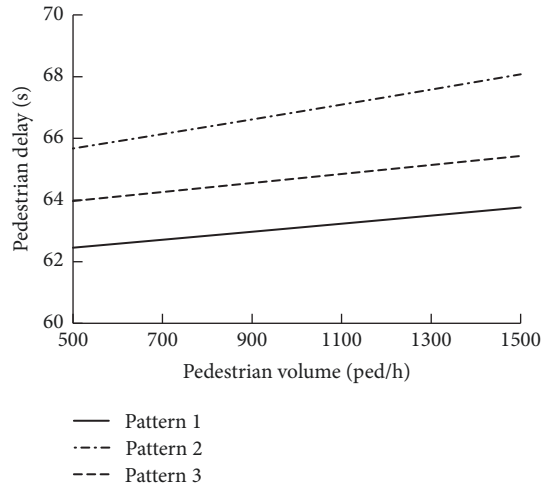

Figure 12: Impact of pedestrian volume.

conflict delay of conventional pattern increases dramatically with the increase of traffic volume and it increases a little in the other two patterns.

The impact of pedestrian volume on pedestrian delay is illustrated in Figure 12. The pedestrian volume is changed from 500 ped/h to 1500 ped/h. It shows a linear growth trend with slight increase intensity. It is due to the fact that the saturation flow rate of the crosswalk is quite large. All the waiting pedestrians can depart in the first several seconds of the green phase.

The impact of the proportion of diagonal crossing on pedestrian delay is shown in Figure 13. The proportion of diagonal crossing is changed from 0.2 to 0.8. It can be found that it has the most effect on conventional pattern. The average pedestrian delay of conventional pattern is the shortest when the proportion of diagonal crossing is less than 0.6 and the average delay of interlaced crossing pattern is the shortest when the proportion of diagonal crossing is from 0.6 to 0.75, while exclusive phase pattern is the shortest when the proportion is more than 0.75.

6. Conclusions

As for three design patterns of pedestrian crossing at the continuous flow intersection, the delay model of different pedestrian flow directions (including through and diagonal crossing) was established, respectively, in this paper according to the characteristics of pedestrian arriving and leaving the intersection. The model was validated by VISSIM simulation. The impact of vehicular volume, pedestrian volume, and the proportion of diagonal crossing on the pedestrian delay in the three patterns were discussed by sensitivity analyses. This provided guidance for decision-makers to better select pedestrian crossing patterns at signalized intersections.

(1) The accuracy of the proposed model for the three design patterns is acceptable. The deviation is less than 3%.

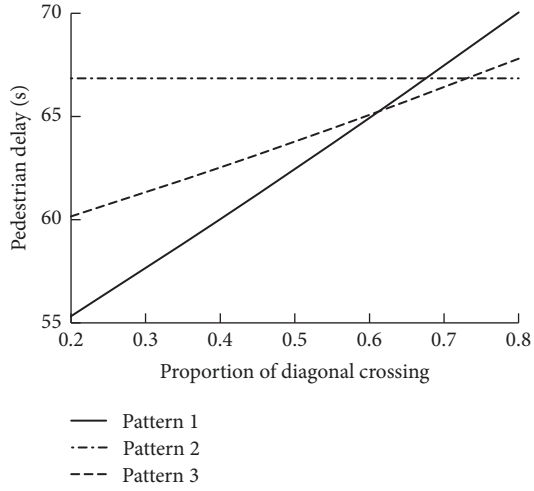

Figure 13: Impact of the proportion of diagonal crossing.

There is no significant difference between the results of the proposed model and that from simulation.

(2) Among these three design patterns, the conventional crossing pattern is mainly applicable to the case of low vehicular and pedestrian volume while the pattern of interlaced pedestrian crossing is mainly applicable to the case of heavy traffic and high pedestrian demand.

(3) Although the exclusive phase pattern is seldom selected as the optimal one (with the shortest delay) in the tested examples, it has the least sensitivity to the change of traffic flow rate and direction ratio, so it is more suitable for the case of high traffic demand volatility.

Please note the proposed delay models are established based on the assumptions that the traffic operates in order and the walking speed and saturation flow rate of pedestrians do not fluctuate, which should be considered in the real-life application. Moreover, the effect of the traffic fluctuation should be considered. Moreover, for the person with vision impairment (blind), it is very important to give them the requisite guidance for crossing, such as the typhlosole, which can be the direction of future work to improve the applicability of the CFIs.

Data Availability

The data used to support the findings of this study are included within the article.

Conflicts of Interest

The authors declare that they have no conflicts of interest.

Acknowledgments

This research is supported by the National Natural Science Foundation of China under Grant no. 51608324.

References

[1] J. E. Hummer, "Unconventional left-turn alternatives for urban and suburban arterials—part one," *ITE Journal (Institute of Transportation Engineers)*, vol. 68, no. 9, pp. 26–29, 1998.

[2] P. Liu, J. J. Lu, and H. Chen, "Safety effects of the separation distances between driveway exits and downstream U-turn locations," *Accident Analysis & Prevention*, vol. 40, no. 2, pp. 760–767, 2008.

[3] A. M. Holzem, J. E. Hummer, C. M. Cunningham, S. W. O'Brien, B. J. Schroeder, and K. Salamati, "Pedestrian and bicyclist accommodations and crossings on superstreets," *Transportation Research Record*, vol. 2486, pp. 37–44, 2015.

[4] J.-P. Moon, Y.-R. Kim, D.-G. Kim, and S.-K. Lee, "The potential to implement a superstreet as an unconventional arterial intersection design in Korea," *KSCE Journal of Civil Engineering*, vol. 15, no. 6, pp. 1109–1114, 2011.

[5] Y. Liu and Z. Luo, "A bi-level model for planning signalized and uninterrupted flow intersections in an evacuation network," *Computer-Aided Civil and Infrastructure Engineering*, vol. 27, no. 10, pp. 731–747, 2012.

[6] J. Zhao, Y. Liu, and T. Wang, "Increasing Signalized Intersection Capacity with Unconventional Use of Special Width Approach Lanes," *Computer-Aided Civil and Infrastructure Engineering*, vol. 31, no. 10, pp. 794–810, 2016.

[7] J. Zhao, Y. Liu, and X. Yang, "Operation of signalized diamond interchanges with frontage roads using dynamic reversible lane control," *Transportation Research Part C: Emerging Technologies*, vol. 51, pp. 196–209, 2015.

[8] R. Jagannathan and J. G. Bared, "Design and operational performance of crossover displaced left-turn intersections," *Transportation Research Record*, no. 1881, pp. 1–10, 2004.

[9] W. Suh and M. P. Hunter, "Signal design for displaced left-turn intersection using Monte Carlo method," *KSCE Journal of Civil Engineering*, vol. 18, no. 4, pp. 1140–1149, 2014.

[10] J. Zhao, W. Ma, H. M. Zhang, and X. Yang, "Increasing the capacity of signalized intersections with dynamic use of exit lanes for left-turn traffic," *Transportation Research Record*, no. 2355, pp. 49–59, 2013.

[11] J. Wu, P. Liu, Z. Z. Tian, and C. Xu, "Operational analysis of the contraflow left-turn lane design at signalized intersections in

China," *Transportation Research Part C: Emerging Technologies*, vol. 69, pp. 228–241, 2016.

[12] J. Zhao and Y. Liu, "Safety evaluation of intersections with dynamic use of exit-lanes for left-turn using field data," *Accident Analysis & Prevention*, vol. 102, pp. 31–40, 2017.

[13] Y. Xuan, C. F. Daganzo, and M. J. Cassidy, "Increasing the capacity of signalized intersections with separate left turn phases," *Transportation Research Part B: Methodological*, vol. 45, no. 5, pp. 769–781, 2011.

[14] W. Ma, H. Xie, Y. Liu, L. Head, and Z. Luo, "Coordinated optimization of signal timings for intersection approach with presignals," *Transportation Research Record: Journal of the Transportation Research Board*, vol. 2013, pp. 93–104, 2013.

[15] C. Yan, H. Jiang, and S. Xie, "Capacity optimization of an isolated intersection under the phase swap sorting strategy," *Transportation Research Part B: Methodological*, vol. 60, pp. 85–106, 2014.

[16] F. D. Mier and B. H. Romo, *Continuous Flow Intersection*, USA, 1991.

[17] W. Hughes, R. Jagannathan, D. Sengupta et al., *Alternative Intersections/Interchanges: Informational Report (AIIR)*, Federal Highway Administration, Washington, DC, USA, 2010.

[18] V. W. Inman, "Evaluation of signs and markings for partial continuous flow intersection," *Transportation Research Record: Journal of the Transportation Research Board*, vol. 2138, no. 1, pp. 66–74, 2009.

[19] L. Tanwanichkul, J. Pitaksringkarn, and S. Boonchawee, "Determining the optimum distance of continuous flow intersection using traffic micro-simulation," *Journal of the Eastern Asia Society for Transportation Studies*, vol. 9, pp. 1670–1683, 2011.

[20] A. Tarko, S. Azam, and M. Inerowicz, "Operational performance of alternative types of intersections - a systematic comparison for indiana conditions," *Congress Proceedings*, vol. 32, no. 31, pp. 386–391, 2010.

[21] M. El Esawey and T. Sayed, "Comparison of two unconventional intersection schemes: Crossover displaced left-turn and upstream signalized crossover intersections," *Transportation Research Record*, no. 2023, pp. 10–19, 2007.

[22] J. Zhao, W. Ma, K. L. Head et al., "Optimal operation of displaced left-turn intersections: a lane-based approach," *Transportation Research Part C: Emerging Technologies*, vol. 61, no. 29, pp. 29–48, 2015.

[23] J. Zhao, Y. Liu, and D. Di, "Optimization model for layout and signal design of full continuous flow intersections," *Transportation Letters*, vol. 8, no. 4, pp. 194–204, 2016.

[24] G.-L. Chang, Y. Lu, and X. Yang, *An Integrated Computer System for Analysis, Selection, and Evaluation of Unconventional Intersections*, Maryland State Highway Administration, Baltimore, Md, USA, 2011.

[25] UDOT, "CFI Guideline: A UDOT Guide to Continuous Flow Intersections," Tech. Rep., Utah Department of Transportation, Salt Lake City, Utah, 2013.

[26] R. Y. Guo and T. Q. Tang, "A simulation model for pedestrian flow through walkways with corners," *Simulation Modelling Practice and Theory*, vol. 21, no. 1, pp. 103–113, 2012.

[27] T.-Q. Tang, H.-J. Huang, and H.-Y. Shang, "A dynamic model for the heterogeneous traffic flow consisting of car, bicycle and pedestrian," *International Journal of Modern Physics C*, vol. 21, no. 2, pp. 159–176, 2010.

[28] C. Yu, W. Ma, K. Han, and X. Yang, "Optimization of vehicle and pedestrian signals at isolated intersections," *Transportation Research Part B: Methodological*, vol. 98, pp. 135–153, 2017.

[29] R. Jagannathan and J. G. Bared, "Design and performance analysis of pedestrian crossing facilities for continuous flow intersections," *Transportation Research Record*, no. 1939, pp. 133–144, 2005.

[30] A. Coates, P. Yi, P. Liu, and X. Ma, "Geometrie and operational improvements at continuous flow intersections to enhance pedestrian safety," *Transportation Research Record*, vol. 2436, pp. 60–69, 2014.

[31] TRB, *Highway Capacity Manual 2010*, Transportation Research Board, Washington, DC, USA, 2010.

[32] X. Guo, M. C. Dunne, and J. A. Black, "Modeling of pedestrian delays with pulsed vehicular traffic flow," *Transportation Science*, vol. 38, no. 1, pp. 86–96, 2004.

[33] J. D. Griffiths, J. G. Hunt, and M. Marlow, "Delays at pedestrian crossings - 4. mathematical models," *Traffic, Engineering and Control*, vol. 26, no. 5, pp. 277–282, 1985.

[34] V. Chilukuri and M. R. Virkler, "Validation of HCM pedestrian delay model for interrupted facilities," *Journal of Transportation Engineering*, vol. 131, no. 12, pp. 939–945, 2005.

[35] M. Kruszyna, P. Mackiewicz, and A. Szydlo, "Influence of pedestrians entry process on pedestrian delays at signal-controlled crosswalks," *Journal of Transportation Engineering*, vol. 132, no. 11, pp. 855–861, 2006.

[36] M. R. Virkler, "Pedestrian compliance effects on signal delay," *Transportation Research Record*, no. 1636, pp. 88–91, 1998.

[37] Q. Li, Z. Wang, J. Yang, and J. Wang, "Pedestrian delay estimation at signalized intersections in developing cities," *Transportation Research Part A: Policy and Practice*, vol. 39, no. 1, pp. 61–73, 2005.

[38] R. Nagraj and P. Vedagiri, "Modeling pedestrian delay and level of service at signalized intersection crosswalks under mixed traffic conditions," *Transportation Research Record*, no. 2394, pp. 70–76, 2013.

[39] X. Ye, J. Chen, G. Jiang, and X. Yan, "Modeling pedestrian level of service at signalized intersection crosswalks under mixed traffic conditions," *Transportation Research Record*, vol. 2512, pp. 46–55, 2015.

[40] T. Tang, Z. Yi, J. Zhang, and N. Zheng, "Modelling the driving behaviour at a signalised intersection with the information of remaining green time," *IET Intelligent Transport Systems*, vol. 11, no. 9, pp. 596–603, 2017.

[41] X. Wang and Z. Tian, "Pedestrian delay at signalized intersections with a two-stage crossing design," *Transportation Research Record*, no. 2173, pp. 133–138, 2010.

[42] J. Zhao and Y. Liu, "Modeling pedestrian delays at signalized intersections as a function of crossing directions and moving paths," *Transportation Research Record*, vol. 2615, no. 1, pp. 95–104, 2018.

[43] P. K. Goh and W. H. K. Lam, "Pedestrian flows and walking speed: A problem at signalized crosswalks," *ITE Journal (Institute of Transportation Engineers)*, vol. 74, no. 1, pp. 28–33, 2004.

[44] J. Y. S. Lee and W. H. K. Lam, "Simulating pedestrian movements at signalized crosswalks in Hong Kong," *Transportation Research Part A: Policy and Practice*, vol. 42, no. 10, pp. 1314–1325, 2008.

[45] K. M. Chen, X. Q. Luo, H. Ji et al., "Towards the pedestrian delay estimation at intersections under vehicular platoon caused conflicts," *Scientific Research and Essays*, vol. 5, no. 9, pp. 941–947, May 2010.